



Inactivation, aggregation, secondary and tertiary structural changes of germin-like protein in *Satsuma mandarina* with high polyphenol oxidase activity induced by ultrasonic processing



Nana Huang^{a,b}, Xi Cheng^{a,b}, Wanfeng Hu^{a,b,*}, Siyi Pan^{a,b}

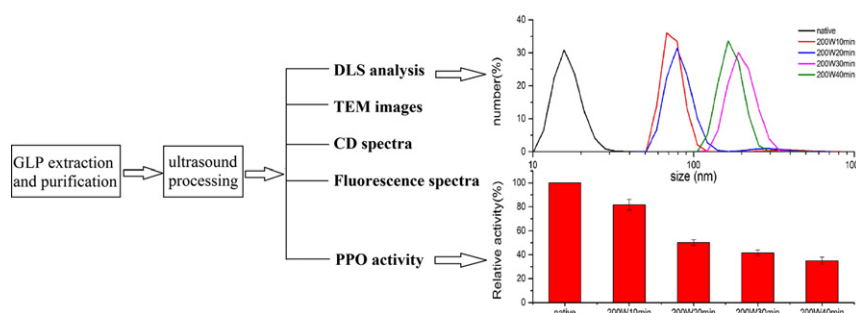
^a College of Food Science and Technology, Huazhong Agricultural University, Wuhan 430070, China

^b Key Laboratory of Environment Correlative Dietology (Huazhong Agricultural University), Ministry of Education, Wuhan, 430070, China

HIGHLIGHTS

- PPO activity of GLP in citrus was significantly inactivated by ultrasonic processing.
- Ultrasound caused GLP particles aggregation and dissociation with process variables.
- Mechanism of PPO inactivation could be protein aggregation and structural changes.

GRAPHICAL ABSTRACT



ARTICLE INFO

Article history:

Received 3 November 2014

Received in revised form 2 December 2014

Accepted 2 December 2014

Available online 10 December 2014

Keywords:

Germin-like protein

Ultrasound

PPO activity

Aggregation, structural change

ABSTRACT

The inhibition of Polyphenol oxidase (PPO) in plants has been widely researched for their important roles in browning reaction. A newly found germin-like protein (GLP) with high PPO activity in *Satsuma mandarina* was inactivated by low-frequency high-intensity ultrasonic (20 kHz) processing. The effects of ultrasound on PPO activity and structure of GLP were investigated using dynamic light scattering (DLS) analysis, transmission electron microscopy (TEM), circular dichroism (CD) spectral measurement and fluorescence spectral measurement. The lowest PPO activity achieved was 27.4% following ultrasonication for 30 min at 400 W. DLS analysis showed ultrasound caused both aggregation and dissociation of GLP particles. TEM images also demonstrated protein aggregation phenomena. CD spectra exhibited a certain number of loss in α -helix structure content. Fluorescence spectra showed remarkable increase in fluorescence intensity with tiny blue-shift following ultrasonication. In conclusion, ultrasound applied in this study induced structural changes of GLP and eventually inactivated PPO activity.

© 2014 Elsevier B.V. All rights reserved.

1. Introduction

Citrus are widely cultivated throughout the tropical and subtropical regions of the world [1]. Citrus fruits are popular worldwide for their pleasant flavor and high nutrition. Browning of citrus fruits during storage and juices processing often causes products deterioration in color, flavor and nutrition. Citrus products browning is usually attributed to non-enzymatic browning caused by chemical reactions such as caramelization, ascorbic acid degradation and the Maillard reaction [2].

Abbreviations: PPO, polyphenol oxidase; GLP, germin-like protein; DLS, dynamic light scattering; TEM, transmission electron microscopy; CD, circular dichroism; Tris, tris(hydroxymethyl)aminomethane; PSD, particle size distribution.

* Corresponding author at: College of Food Science and Technology, Huazhong Agricultural University, No.1, Shi Zi Shan Road, Wuhan 430070, P. R of China. Tel.: +86 15071368563.

E-mail address: wanfenghu@mail.hzau.edu.cn (W. Hu).

However, many fruits and vegetables exhibit serious enzymatic browning, such as bananas, apples and potatoes. Enzymatic browning is usually induced by polyphenol oxidase, which catalyze the oxygen-dependent oxidation of phenols to quinones, finally causing quality loss of fruits and vegetables [3] and [4]. Although citrus fruits have high levels of acid, especially ascorbic acid, which is reported to be good inhibitors of enzymatic browning [5], the browning reaction would not be stopped until all enzymes had been deactivated. Therefore, all PPO activity should be included when considering enzymatic browning.

A newly found germin-like protein in *Satsuma mandarine* was reported to have high PPO activity [6], with the kinetic constants being 0.0365 M and 0.0196 M for catechol and pyrogallol as substrates respectively. Even though the protein was extracted from citrus peels, it is easily to be mixed within juices during processing. Since citrus fruits contains abundant phenolic compounds [7], the newly found GLP with high PPO activity may be responsible for diminished quality of citrus juices.

Recently, low-frequency high-intensity ultrasound in the kHz range has been investigated as a new technology in food industry. Ultrasound was applied to induce novel changes in the physicochemical properties of foods in various areas [8], such as nanoemulsion preparation [9], ultrasound-assisted extraction [10] and improvement of foaming properties [11]. Furthermore, food technologists have tried to use ultrasound to alter enzyme activities such as pectinmethylesterase [12], polyphenoloxidases [13] and peroxidases [14] responsible for deterioration of fruit and vegetable juices. As an efficient way to inactivate enzymes, ultrasonic processing was reported to have no detrimental effect on the quality of fruits juices such as orange juice [15] and grape juice [16]. The inactivation effect of ultrasound is mainly attributed to a phenomenon called cavitation [17]. When ultrasound travels through a liquid, tiny gas bubbles will form, grow and collapse due to pressure changes [14]. Bubble implosion generates extreme physical phenomena (temperatures over 1000 K and pressures up to 500 MPa) and very high shear forces at micro-scale [14].

Up to date, inactivation of PPO activity in citrus has rarely been investigated. According to our previous study [6], the relative PPO activity of GLP at 85 °C for 5 min was even a little higher than GLP at 25 °C for 5 min, indicating that thermal treatment had weak effect on inhibiting PPO activity of GLP. On the other hand, in food industry, thermal effect, which may result in the loss of food color, flavor and nutrition, should be avoided. Thus, the object of this study was to evaluate the impact of low-frequency high-intensity ultrasonic processing on the PPO activity and structural changes of GLP purified from *Satsuma mandarine* peel. The structural analysis was conducted using DLS analysis, TEM, CD spectral measurement and fluorescence spectral measurement, aiming to exploring the mechanism of ultrasonic processing on enzyme activity.

2. Materials and methods

2.1. Materials and reagents

Freshly harvested citrus fruits (*S. mandarine*) were purchased in Wenzhou, China, in November 2013. The peels were separated from the fruits, dried under the sun, and stored at 4 °C until used. Tris(hydroxymethyl)aminomethane (Tris), crosslinking polyvinylpyrrolidone, ammonium sulfate, pyrogallol were purchased from Sigma Chemical Co. (St. Louis, USA). All chemicals and reagents used were of analytical grade purity. DEAE Sepharose Fast Flow and Sephacryl S200 resin were obtained from GE Healthcare (Milan, Italy). Water used in buffers were purified with the Milli-Q purification system (Millipore Iberica, Madrid, Spain).

2.2. Protein extraction and purification

The extraction and purification methods were done according to our previous work [6]. Proteins were precipitated with 80% saturated

ammonium sulfate, dialyzed against 0.5 M Tris-HCl buffer (pH 7.0), then concentrated using an ultrafilter (Millipore Co., Bedford, MA, USA) and loaded onto a DEAE Sepharose Fast Flow column (1.6 × 30 cm), which were pre-equilibrated with 0.05 M Tris-HCl buffer (pH 7.0). Fractions with the highest PPO activity were collected and stored at 4 °C.

2.3. Ultrasonic processing

A 1000 W ultrasonic processor (JY92-2D, Ningbo Scientz Biotechnology Co.Ltd, Ningbo, China) with a 0.636 cm diameter probe tip was used for ultrasonic treatments. The processing was carried out at 20 kHz frequency with pulse durations of 5 s on and 5 s off. The samples were kept in ice-water bath when treated with ultrasound to maintain the low temperature. 10 mL protein solutions were prepared in a 25 ml centrifugal tube for sonication. Experiments were set to investigate the effect of ultrasonic time (10, 20, 30, 40 min at 200 W) and intensity (100, 200, 400 W for 30 min) on GLP. Then all samples treated with ultrasound were collected for structural and PPO activity analysis. All treatments were carried out in triplicate.

2.4. Polyphenol oxidase (PPO) activity determination

The PPO activity of native and ultrasonic treated GLPs was assayed by monitoring the increase in absorbance at 420 nm for pyrogallol with a UV1800 spectrophotometer (Shimadzu, Kyoto, Japan). The assay was performed according to Cheng et al. [6] with some modifications. 0.7 mL of protein solutions (0.067 mg/mL) were added to 1.8 mL of 0.1 M pyrogallol dissolved in 0.1 M Tris-HCl buffer (pH 7.0), then the initial linear increase rate at 420 nm was recorded. One unit of the enzyme activity was defined as the amount of the enzyme that increases 0.001 of absorbance per minute per milligram of protein solution. In this study, the relative PPO activity of GLP was calculated using the following formula:

$$\text{Relative PPO activity} = \frac{\text{PPO activity of ultrasonic treated GLP}}{\text{PPO activity of native GLP}} \times 100\%$$

2.5. Dynamic light scattering (DLS) analysis

The particle size measurement was performed using a Zetasizer Nano-ZS device (Malvern Instruments, Malvern, Worcestershire, U.K.). Native and ultrasonic treated protein solutions were prepared at ambient temperature in 50 mM Tris-HCl buffer (pH 6.8). The protein particle size and distribution were reported as the mean and standard deviation of at least five readings. All measurements were carried out in triplicate.

2.6. Transmission electron microscopy analysis

The electron microscopy was done at state key laboratory of virology in Wuhan, China. Proteins in 50 mM Tris-HCl buffer (pH 6.8) were used for measurement. Electron microscopy (TEM) images of native and ultrasonic treated protein solutions were obtained using a 100 kV transmission electron microscope at 75 kV excitation voltage (HITACHI-H7000FA, Hitachi Limited).

2.7. Circular dichroism spectral measurement

Circular dichroism (CD) spectra of native and ultrasonic treated protein solutions were recorded with a JASCO J-1500 spectropolarimeter (Japan Spectroscopic Co., Tokyo, Japan), using a quartz cell of 1 mm path length at ambient temperature. The protein samples of 0.067 mg/mL were prepared in 50 mmol/L Tris-HCl buffer (pH 6.8), using protein-free buffer as the blank. CD spectra were scanned in the far-ultraviolet range from 196 to 260 nm. The scan speed was

100 nm/min with a bandwidth of 1 nm. The CD data were expressed in terms of mean residue ellipticity, $[\theta]$, in $\text{deg cm}^2 \text{dmol}^{-1}$. The secondary structure contents were derived from Yang's equation [18].

2.8. Fluorescence spectral measurement

Intrinsic fluorescence spectra of native and ultrasonic treated protein solutions were performed at ambient temperature using a F-4600 Fluorescence spectrophotometer (Hitachi, Japan). Protein solutions (0.067 mg/mL) in 50 mM Tris-HCL (pH 6.8) were measured at 350 nm emission wavelength to obtain the maximum excitation wavelength. Then the protein solutions were scanned at the maximum excitation wavelength to record all of the emission spectra. The excitation spectrum: λ_{ex} :280 nm and λ_{em} :300–400 nm; Both Em slit and Ex slit were set as 2.5 nm; scan speed was set as 200 nm/min.

3. Results and discussion

3.1. Effect of ultrasonic processing on the PPO activity of GLP

The relative PPO activity for GLPs subjected to different ultrasonic time (10, 20, 30, 40 min at 200 W) and intensity (100, 200, 400 W for 30 min) is displayed in Fig. 1(a) and (b), respectively. As it is shown, the PPO activity of GLP was gradually reduced with increasing ultrasonic time and intensity. The lowest PPO activity was 27.4%, achieved at ultrasonic treatment for 30 min at 400 W. Previous studies showed inverse and limited inhibitory effect of ultrasound on PPO activity [13] and [19]. However, protein in our research was identified as a kind of germin-like protein rather than a genuine PPO as in these two studies. The peptide sequences and overall structures of the two proteins are different [6 and 20]. Moreover, the samples used in their studies for ultrasonic processing were apple discs (5 mm thick, 15 mm diameter) and crude PPO extract of mushroom, respectively. The reasons could be ascribed to sample preparation difference because we collected purified protein solution for ultrasonic processing. Thus, these purified proteins could be more likely to suffer from ultrasonic processing without protection from surrounding substances.

The decrease in enzyme activity probably could be attributed to the high levels of pressure, temperature, shear forces and free radicals through sonolysis of water generated by the ultrasonic treatment [14 and 21]. Generally, longer ultrasonic time and higher ultrasonic intensity resulted in lower PPO activity. Mechanisms involved in these changes may be longer time, and higher intensity transmits more ultrasonic energy to the protein solutions, which may induce higher levels of protein denaturation.

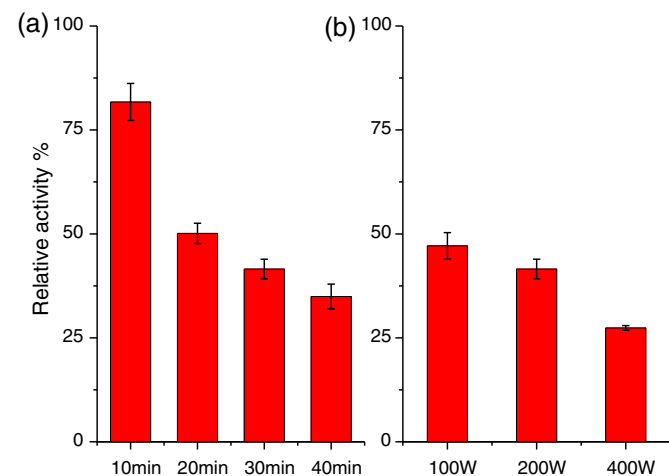


Fig. 1. The relative PPO activity of ultrasonic treated GLP. (a) Ultrasonic processing at 200 W for 10, 20, 30, 40 min. (b) Ultrasonic processing for 30 min at 100, 200, 400 W.

The PPO activity of native GLP was 4254 ± 154 U/mg/min (shown in Table 1), indicating strong ability to catalyze browning reaction. Even though GLPs blended in citrus juices might be in low concentration, their high PPO activity could lead to partly browning of juices. Even though the reported individual effect of ultrasound on PPO activity was poor, they did demonstrated synergistic effect with ascorbic acid [13] and heat [19]. Considering the high acid content in citrus fruits and heat sterilization in juices processing, simultaneous treatment combined ultrasound with heat could be more efficient.

3.2. DLS analysis of GLPs treated with ultrasound

Fig. 2 shows the particle size distribution (PSD) of the native and ultrasonic treated GLP using DLS analysis. As it is shown, the peak diameter of native GLP is 15.7 nm with the peak value of 30.8 in number fraction. The PSD pattern of native GLP exhibited a relatively narrow span of 16.5 nm.

The effect of ultrasonic time (10, 20, 30, 40 min at 200 W) on GLP (shown in Fig. 2a) exhibited initial increase and eventual decrease in peak particle size. With ultrasonic treated for 10 min, the peak particle diameter increased to 68.1 nm with the diameter span increased to 46.9 nm. The maximum peak particle size (190.1 nm) and diameter span (219.6 nm) were obtained with ultrasonic time increased to 30 min. These changes suggested that ultrasound in aqueous system could promote interactions of protein molecules, leading to parts of these molecules aggregating and forming some larger particles. However, after treated for 40 min, the peak diameter slightly decreased to 164.2 nm with a narrowed span of 132.6 nm. Ultrasonic processing for this time long probably caused some larger particles dissociated into smaller ones.

The effect of ultrasonic intensity (100 to 400 W) on the PSD pattern of GLP subjected to ultrasonic treatment for 30 min are shown in Fig. 2b. As it is shown, the peak diameter together with the diameter span of ultrasonic treated GLP increased following the increase of ultrasonic intensity. The maximum peak diameter (255.0 nm) and span (294.5 nm) was achieved after ultrasonic treated at 400 W for 30 min.

In general, all proteins subjected to ultrasonic processing achieved much larger particle size compared to the native GLP. GLP particles firstly aggregated then some larger aggregates dissociated following the increase of ultrasonic time. Ultrasound induced protein aggregation and dissociation has been reported previously. Sonicated porcine fumarase appears as fibrous aggregates with a very regular rod-like shape of variable size and thickness [22]. The particle size of bovine serum albumin increased up to 3.4 times after 90 min of sonication [23]. Defatted wheat germ proteins were reported to dissociate into smaller size particles after ultrasonic pretreatment [24]. Proteins may be destabilized at the air-liquid interface of ultrasonic-induced bubbles [25], resulting in the aggregation and homogenization of protein particles. The native structure of proteins, including the subtle balance between many non-covalent interactions, can be easily disrupted by ultrasonic processing, resulting in protein denaturation and aggregation [25]. Furthermore, protein aggregates formed by the non-covalent interactions between protein molecules such as electrostatic and hydrophobic interactions

Table 1
Secondary structure contents and PPO activity of native and ultrasonic treated GLP.

Ultrasonic processing	Secondary structure contents (%)				PPO activity (U/mg/min)
	α -Helix	β -Sheet	β -Turn	Random coil	
Native GLP	40.4	0	10.6	49	4254 ± 154
200 W 10 min	39.1	0	13	47.9	3473 ± 63
200 W 20 min	32.5	0	20.1	47.4	2130 ± 27
200 W 30 min	31.6	0	26.6	41.8	1765 ± 36
200 W 40 min	29.9	0	28.2	41.9	1484 ± 72
100 W 30 min	36.8	18.9	0	44.3	2002 ± 63
400 W 30 min	35.6	0	6	58.4	1164 ± 18

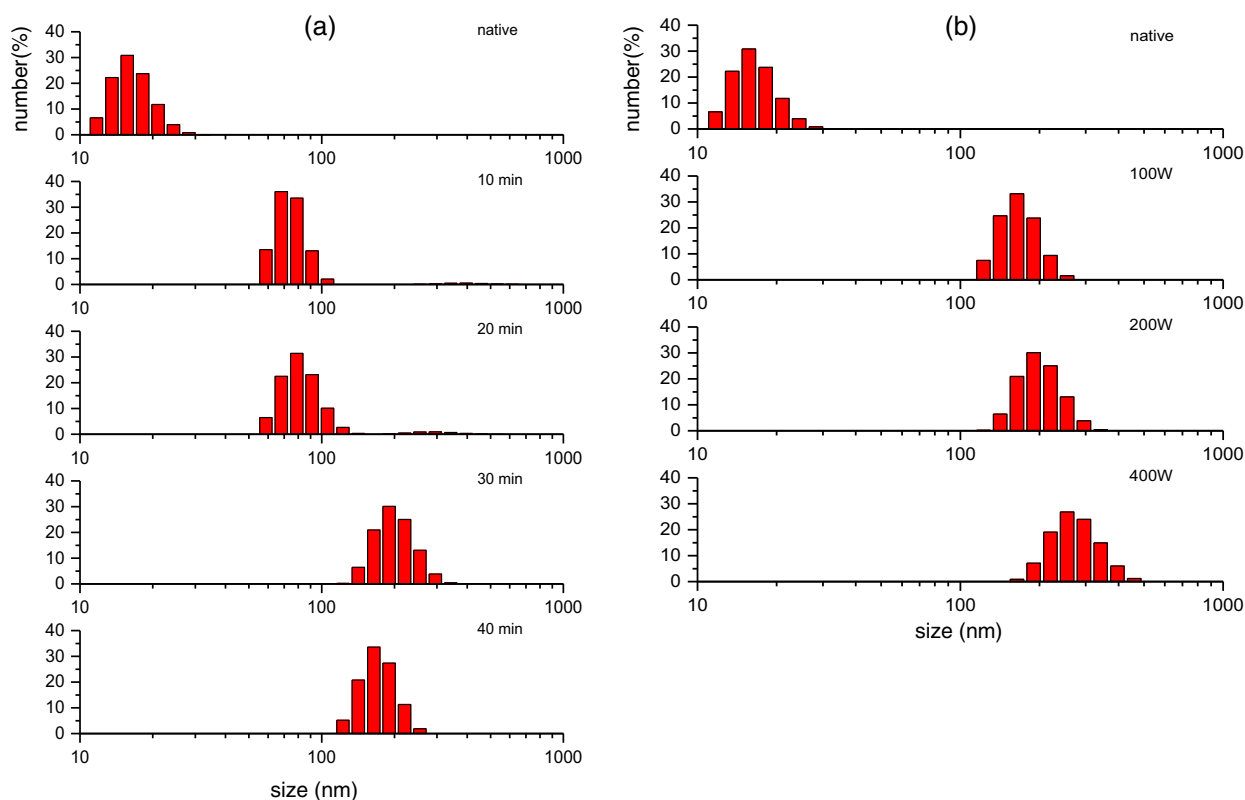


Fig. 2. Particle size distribution of native and ultrasonic treated GLP. (a) Ultrasonic processing at 200 W for 10, 20, 30, 40 min. (b) Ultrasonic processing for 30 min at 100, 200, 400 W.

[26] could be cut off with excessive ultrasonic duration, leading to GLP aggregates particle breakage.

Combining the changes in PPO activity and PSD patterns of GLPs, all ultrasonic treated GLPs exhibited reduced activity along with gradually increased particle size. The original state of GLPs in aqueous system may be more suitable for catalytic reactions. Meanwhile, proteins aggregated together may have their inner structure hindered to interact with substrates for catalytic reaction.

3.3. Microstructure analysis of GLPs treated with ultrasound

The microstructures of native and ultrasonic treated GLP examined by transmission electron microscopy are displayed in Fig. 3. The microstructure of native GLP (shown in Fig. 3 a) seems to be monodisperse with the protein particle size mostly around 20 nm. Fig. 3 b and c shows the microstructure of ultrasonic treated GLP for 10 min and 30 min at 200 W, with the primarily particle size approximately 100 nm and 200 nm, respectively. The images also show that GLPs subjected to ultrasonic processing formed a number of ball-shaped aggregates with much larger particle size. Moreover, the protein aggregates grew bigger following the increase of ultrasonic time and intensity. These aggregation phenomena are consistent with the results showed in DLS analysis. However, the dissociation phenomenon obtained in DLS could not be clearly seen through the TEM images. The result was acceptable considering the sample pretreatment difference when using these two measuring instruments as well as the tiny difference between the two PSD patterns.

3.4. CD spectroscopy analysis of GLPs treated with ultrasound

The secondary structures of GLPs in Tris-HCl buffer were analyzed through CD spectroscopy. It is a useful method to monitor the conformational changes of protein by CD spectral measurement [21].

The CD spectra of the native and ultrasonic treated GLP are shown in Fig. 4. Two double-negative slots at 208 and 222 nm of the native GLP were characterized as typical α -helix conformation in the secondary structure [27 and 28]. The α -helix content in native GLP was identified as 40.4%. Generally, the value of the slots decreased in all samples subjected to ultrasonic processing. These changes suggested that ultrasound triggered α -helix conformation loss in the secondary structure of GLP [21 and 29]. In general, values of the two slots gradually decreased following the increasing of ultrasonic time and intensity. The secondary structure of a protein depends not only on the local amino acids sequence but also on the interactions of different part of molecular. Therefore, the interactions of protein molecules probably were disrupted by ultrasonic processing, although some of the spectral changes were not so significant.

The contents of α -helix, β -sheet, β -turn and random coil together with PPO activity of native and ultrasonic treated GLP are shown in Table 1. It can be seen that α -helix decreased with a concomitant increase in β -structure after ultrasonic treatment. The results were consistent with the findings reported by Stathpoulos et al. [25]. They studied a range of structurally diverse proteins aggregates induced by sonication and found that sonication-induced aggregates have high β -structure contents, and proteins with significant native α -helical structure show increased β -structure in the aggregates. However, proteins subjected to ultrasonic for 30 min at 400 W exhibited a large number of decrease in β -structure content and a little decrease in α -helix content accompanied by high random coil content of 58.4%, making the proteins much softer and more flexible. Meanwhile, the enzyme activity at this treatment was the lowest among all, suggesting that the regular and tight structure of proteins was more favorable for catalytic reaction.

PPOs primarily consist of α -helical conformation with the catalytic center surrounded by four α -helix bundles [30 and 31]. Thus, the high content of α -helix GLP may constitute the helix bundles of catalytic center which is responsible for PPO activity. Ultrasound caused α -helix conformation loss, resulting in the inactivation of PPO activity of GLP [32].

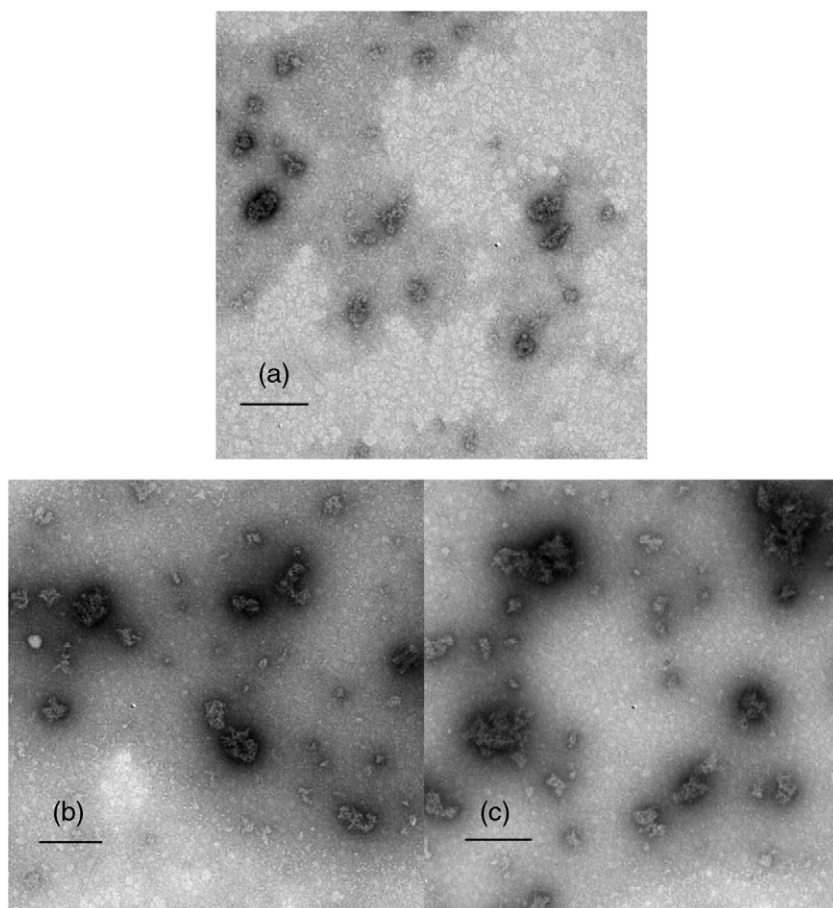


Fig. 3. TEM images of native and ultrasonic treated GLP (markers in the three pictures represent 200 nm) (a) native GLP. (b) Ultrasonic processing at 200 W for 10 min. (c) Ultrasonic processing at 200 W for 30 min.

3.5. Fluorescence spectroscopy analysis of GLPs treated with ultrasound

In this study, the fluorescence properties of native and ultrasonic treated GLPs were examined by fluorescence spectroscopy. Fluorescence

spectral is a useful technique to follow tertiary structure transition in proteins because the intrinsic fluorescence of aromatic amino acid residues is sensitive to the polarity of microenvironment [33]. The fluorescence spectrum is mainly attributed to Trp, Tyr and Phe residues,

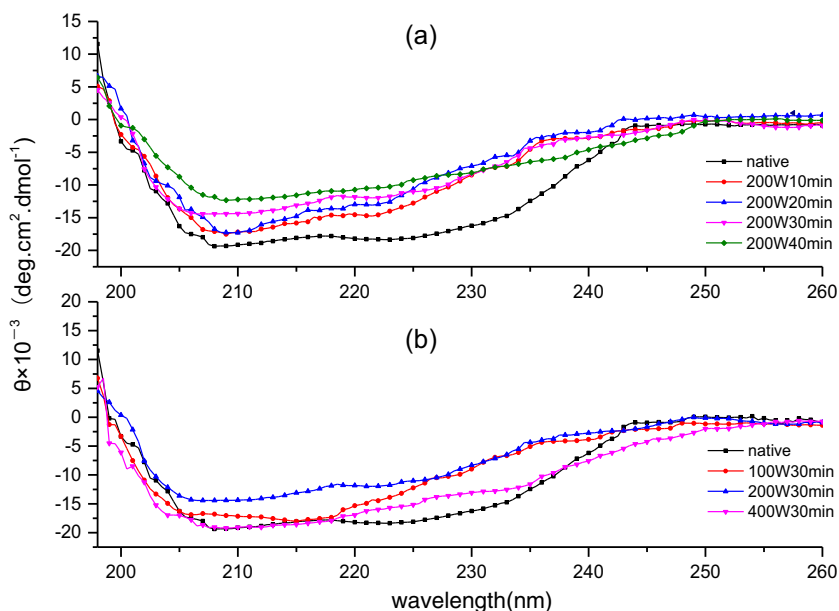


Fig. 4. CD spectra of native and ultrasonic treated GLP. (a) Ultrasonic processing at 200 W for 10, 20, 30, 40 min. (b) Ultrasonic processing for 30 min at 100, 200, 400 W.

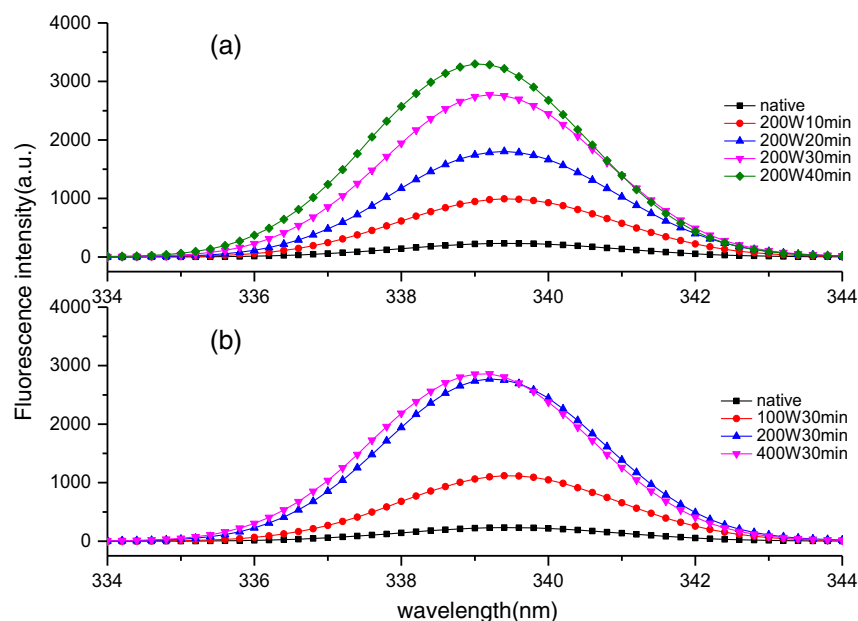


Fig. 5. Fluorescence spectra of native and ultrasonic treated GLP. (a) Ultrasonic processing at 200 W for 10, 20, 30, 40 min. (b) Ultrasonic processing for 30 min at 100, 200, 400 W.

particularly the Trp residue [34]. The observed maximum emission wavelength (λ_{\max}) for Trp residues in proteins ranges from 308 to 355 nm [35].

Fig. 5 shows the fluorescence spectra of native and ultrasonic treated GLP. The λ_{\max} of native GLP is 339 nm with the fluorescence intensity of 231.4, suggesting that Trp residues in GLP were located in non-polar hydrophobic environment.

The effect of ultrasonic time (10, 20, 30, 40 min at 200 W) on fluorescence spectra of GLP are shown in Fig. 5 a. As it is shown, all samples subjected to ultrasonic processing exhibited remarkable increase in fluorescence intensity compared to native GLP. Ma et al. [21] also reported increased fluorescence intensity of alcalase after ultrasonic treatment at 80 W for 4 min at 20 kHz. With the increase of ultrasonic time, the fluorescence intensity gradually increased. The peak fluorescence intensity value increased from 231.4 (native GLP) to 3301 (ultrasonic treated for 40 min at 200 W). As to λ_{\max} , 0.2 and 0.4 nm blue shifts were observed after 30 min and 40 min treatment, respectively. Fig. 4 b exhibits similar trend of the effect of ultrasonic intensity (100, 200, 400 W for 30 min) on fluorescence spectra of GLP. Fluorescence spectra of samples treated at 400 W did not show significant difference with proteins treated at 200 W.

The increase in emission intensity of ultrasonic treated GLP indicated that some chromophores were relocated into less polar microenvironment. This may reflect that some Trp residues may have been associating within non-polar region because of polymerization, aggregation or peptide–peptide association, consequently leading to the increase in relative fluorescence intensity [34].

The slight blue shifts (the maximum of 0.4 nm) of ultrasonic treated GLP indicated that ultrasound induced Trp residues buried a little more inside the protein, as the more buried Trp residues the more the blue shifts [35]. The fluorescence quantum yield of aromatic amino acid residues decreases with the increase of their exposure to solvent [24]. Therefore, the fluorescence quantum yield of these residues may be increased for been buried more deeply inside the protein, resulting in largely increased fluorescence intensity.

As more amino acid residues buried inside ultrasonic treated GLPs, the tertiary structure conformation of proteins will be less favorable for the substrates contacting with the enzyme catalytic center. Thus, the ultrasonic treated GLPs demonstrated reduced PPO activity.

4. Conclusion

In this study, low-frequency high-intensity ultrasound showed strong inactivation effect on PPO activity of GLP. Moreover, the relative activity decreased following the increase of ultrasonic time and intensity. The mechanisms involved in could be protein aggregation, denaturation in secondary and tertiary structure. Aggregated proteins might form the structure less favorable for contact with substrates. The subsequent conformational changes with loss of α -helical content and more buried amino acid residues made the catalytic center less matchable for reaction with substrates.

Acknowledgments

The authors were grateful to be supported by the National Natural Science Foundation of China (No. 31401507) and Specialized Research Fund for the Doctoral Program of Higher Education of China (52902-0900206141).

References

- [1] M. Talon, F.G. Gmitter, Citrus genomics, *Int. J. Plant Genom.* (2008), <http://dx.doi.org/10.1155/2008/528361>.
- [2] S.S. Bharate, S.B. Bharate, Non-enzymatic browning in citrus juice: chemical markers, their detection and ways to improve product quality, *J. Food Sci. Technol.* 51 (10) (2014) 2271–2288.
- [3] Y. Jiang, Role of anthocyanins, polyphenol oxidase and phenols in lychee pericarp browning, *J. Sci. Food Agric.* 80 (2000) 305–310.
- [4] L. Vámos-Vigyázó, N.F. Haard, Polyphenol oxidases and peroxidases in fruits and vegetables, *Crit. Rev. Food Sci. Nutr.* 15 (1) (1981) 49–127.
- [5] M. Landi, E. Degl'Innocenti, L. Guglielminetti, L. Guidi, Role of ascorbic acid in the inhibition of polyphenol oxidase and the prevention of browning in different browning-sensitive *Lactuca sativa* var. capitata (L.) and *Eruca sativa* (Mill.) stored as fresh-cut produce, *J. Sci. Food Agric.* 93 (8) (2013) 1814–1819.
- [6] X. Cheng, X. Huang, S. Liu, M. Tang, W. Hu, S. Pan, Characterization of germin-like protein with polyphenol oxidase activity from Satsuma mandarin, *Biochem. Biophys. Res. Commun.* 449 (3) (2014) 313–318.
- [7] A. Bocco, M. Cuvelier, H. Richard, C. Berset, Antioxidant activity and phenolic composition of citrus peel and seed extracts, *J. Agric. Food Chem.* 46 (6) (1998) 2123–2129.
- [8] F. Chemat, Zill-E-Huma, M.K. Khan, Applications of ultrasound in food technology: processing, preservation and extraction, *Ultrason. Sonochem.* 18 (4) (2011) 813–835.
- [9] J.A. Cárcel, J.V. García-Pérez, J. Benedito, A. Mulet, Food process innovation through new technologies: use of ultrasound, *J. Food Eng.* 110 (2) (2012) 200–207.
- [10] Y. Picó, Ultrasound-assisted extraction for food and environmental samples, *TrAC Trends Anal. Chem.* 43 (2013) 84–99.

- [11] K.D. Martínez, C.C. Sanchez, New view to obtain dryer food foams with different polysaccharides and soy protein by high ultrasound, *Int.J. Carbohydr. Chem.* (2014), <http://dx.doi.org/10.1155/2014/259356>.
- [12] P. Raviyan, Z. Zhang, H. Feng, Ultrasonication for tomato pectinmethylesterase inactivation: effect of cavitation intensity and temperature on inactivation, *J. Food Eng.* 70 (2) (2005) 189–196.
- [13] J.-H. Jang, K.-D. Moon, Inhibition of polyphenol oxidase and peroxidase activities on fresh-cut apple by simultaneous treatment of ultrasound and ascorbic acid, *Food Chem.* 124 (2) (2011) 444–449.
- [14] S.S. Ercan, C. Soysal, Effect of ultrasound and temperature on tomato peroxidase, *Ultrason. Sonochem.* 18 (2) (2011) 689–695.
- [15] M. Valero, N. Recrosio, D. Saura, N. Muñoz, N. Martí, V. Lizama, Effects of ultrasonic treatments in orange juice processing, *J. Food Eng.* 80 (2) (2007) 509–516.
- [16] L.N. Lieu, V.V.M. Le, Application of ultrasound in grape mash treatment in juice processing, *Ultrason. Sonochem.* 17 (1) (2010) 273–279.
- [17] C.P. O'Donnell, B.K. Tiwari, P. Bourke, P.J. Cullen, Effect of ultrasonic processing on food enzymes of industrial importance, *Trends Food Sci. Technol.* 21 (7) (2010) 358–367.
- [18] K.S. Kim, S. Kim, H.J. Yang, D.Y. Kwon, Changes of glycinin conformation due to pH, heat and salt determined by differential scanning calorimetry and circular dichroism, *Int. J. Food Sci. Technol.* 39 (4) (2004) 385–393.
- [19] X.f Cheng, M. Zhang, B. Adhikari, The inactivation kinetics of polyphenol oxidase in mushroom (*Agaricus bisporus*) during thermal and thermosonic treatments, *Ultrason. Sonochem.* 20 (2) (2013) 674–679.
- [20] A.M. Mayer, Polyphenol oxidases in plants and fungi: going places? A review, *Phytochemistry* 67 (21) (2006) 2318–2331.
- [21] H. Ma, L. Huang, J. Jia, R. He, L. Luo, W. Zhu, Effect of energy-gathered ultrasound on Alcalase, *Ultrason. Sonochem.* 18 (1) (2011) 419–424.
- [22] M. Barteri, M. Diociaiuti, A. Pala, S. Rotella, Low frequency ultrasound induces aggregation of porcine fumarase by free radicals production, *Biophys. Chem.* 111 (1) (2004) 35–42.
- [23] I. Gülseren, D. Güzey, B.D. Bruce, J. Weiss, Structural and functional changes in ultrasonicated bovine serum albumin solutions, *Ultrason. Sonochem.* 14 (2) (2007) 173–183.
- [24] J. Jia, H. Ma, W. Zhao, Z. Wang, W. Tian, L. Luo, R. He, The use of ultrasound for enzymatic preparation of ACE-inhibitory peptides from wheat germ protein, *Food Chem.* 119 (1) (2010) 336–342.
- [25] P.B. Stathopoulos, G.A. Scholz, Y. Hwang, J.A.O. Rumfeldt, J.R. Lepock, E.M. Meiering, Sonication of proteins causes formation of aggregates that resemble amyloid, *Protein Sci.* 13 (11) (2004) 3017–3027.
- [26] W. Visessanguan, M. Ogawa, S. Nakai, H. An, Physicochemical changes and mechanism of heat-induced gelation of arrowtooth flounder myosin, *J. Agric. Food Chem.* 48 (4) (2000) 1016–1023.
- [27] S.M. Kelly, N.C. Price, The application of circular dichroism to studies of protein folding and unfolding, *Biochim. Biophys. Acta* 1338 (2) (1997) 161–185.
- [28] S.M. Kelly, T.J. Jess, N.C. Price, How to study proteins by circular dichroism, *Biochim. Biophys. Acta* 1751 (2) (2005) 119–139.
- [29] W. Hu, Y. Zhang, Y. Wang, L. Zhou, X. Leng, X. Liao, X. Hu, Aggregation and homogenization, surface charge and structural change, and inactivation of mushroom tyrosinase in an aqueous system by subcritical/supercritical carbon dioxide, *Langmuir* 27 (3) (2011) 909–916.
- [30] H. Decker, T. Schweikardt, F. Tuczek, The first crystal structure of tyrosinase: all questions answered? *Angew. Chem. Int. Ed. Engl.* 45 (28) (2006) 4546–4550.
- [31] T. Klabunde, C. Eicken, J.C. Sacchettini, B. Krebs, Crystal structure of a plant catechol oxidase containing a dicopper center, *Nat. Struct. Biol.* 5 (12) (1998) 1084–1090.
- [32] R. Li, Y. Wang, W. Hu, X. Liao, Changes in the activity, dissociation, aggregation, and the secondary and tertiary structures of a thaumatin-like protein with a high polyphenol oxidase activity induced by high pressure CO₂, *Innov. Food Sci. & Emerg. Technol.* 23 (2014) 68–78.
- [33] M.I. Viseu, T.I. Carvalho, S.M.B. Costa, Conformational transitions in beta-lactoglobulin induced by cationic amphiphiles: equilibrium studies, *Biophys. J.* 86 (4) (2004) 2392–2402.
- [34] C. Tang, X.Q. YANG, Z. Chen, H. Wu, Z.Y. PENG, Physicochemical and structural characteristics of sodium caseinate biopolymers induced by microbial transglutaminase, *J. Food Biochem.* 29 (4) (2005) 402–421.
- [35] R.W. Alston, M. Lasagna, G.R. Grimsley, J.M. Scholtz, G.D. Reinhart, C.N. Pace, Tryptophan fluorescence reveals the presence of long-range interactions in the denatured state of ribonuclease Sa, *Biophys. J.* 94 (6) (2008) 2288–2296.